Journal of Materials and Environmental Sciences
ISSN : 2028-2508
CODEN : JMESCN

Copyright © 2018,
University of Mohammed Premier
Oujda Morocco

J. Mater. Environ. Sci., 2018, Volume 9, Issue 3, Page 994-1002

https://doi.org/10.26872/jmes.2018.9.3.114

http://www.jmaterenvironsci.com

Synthesis, physicochemical, thermal, computationand DNA binding evaluation of *trans*-[$CuBr_2(Me_2NCH_2CH_2NH_2)_2$] complex

Muneer Abdoh[1]*, Reeta Essa[2], Ashraf Sawafta[2]*, Mohammed Al-Nuri[3], Aminah Abu Libdeh[2], Anas Al Ali[3], Nabil Al-Zaqri[4], Karthik Kumara[5], Abdelkader Zarrouk[6], Ismail Warad[3]*

[1]*Department of Physics, Science College, An-Najah National University, P.O. Box 7, Nablus, Palestine*
[2] *Biology and Biotechnology Department, An-Najah National University, P.O. Box 7, Nablus, Palestine*
[3]*Department of Chemistry, AN-Najah National University P.O. Box 7, Nablus, Palestine*
[4]*Department of Chemistry, College of Science, King Saud University, P.O. Box 2455, Riyadh 11451, Saudi Arabia*
[5]*Department of Studies in Physics, University of Mysore, Manasagangotri, Mysore - 570 006, India*
[6]*LCAE-URAC18, Faculté des Sciences d'Oujda, Université Mohammed Premier, BP 4808, 60046 Oujda, Morocco*

Received04Oct 2017,
Revised 01Nov 2017,
Accepted 10 Nov 2017

Keywords
- ✓ Copper(II),
- ✓ Spectral,
- ✓ DFT,
- ✓ Thermal,
- ✓ DNA binding.

warad@najah.edu
Fax: 0097092345982

Abstract

Asymmetrical $Me_2NCH_2CH_2NH_2$/copper(II)/bromide complex was synthesized in a good yield under ultrasonic vibration mode. The desired complex was characterized using, elemental EA, conductometric, UV-Vis, FTIR, MS and EDX analysis. The thermal behaviour of the complex was performed by TG. DFT calculations in order to investigate the complex structure parameters. The absorption and viscosity titration measurements reflected the desired complex as strong intercalate DNA-binder with high K_b binding constant value.

1. Introduction

Copper(II)/diamine/X_2 complexes are considered to be vital class of complexes because of their applications in several science fields [1-5]. They can be considered as simple models to understand the medical behaviour of Cu-proteins unit [6-11]. The chromotropic behaviour of Cu^{II}(NN) complexes have attracted much attention due to the potentially colorimetric applications of such complexes like: indicators, thermochromic paints and temperature sensors [9-11].

Many Cu(II) complexes of N-ligands acted as antimicrobial and anticancer agents [6-9]. Cu:DNA binding studies play a critical role in development of novel therapeutic anti-cancer reagents [5, 8, 10].

Currently, huge number of Cu(II)/N-donors complexes being used as DNA binders in order to develop new anti-cancer chemotherapy [4-12]. Recently, we have prepared several ligands and their metal ion Cu(II) complexes. The structures of these complexes mostly were analysed by single-crystal XRD, FTIR, and UV-vis. High level of computationalanalysis were performed to find structural relations between DFT and XRD data. Additionally, the biological applications like DNA-binding, anti-cancer and anti-bacterial activity of these complexes were carried out [12-17].

In this paper, we report the structural characterization and theoretical investigation of *Trans*-[$CuBr_2(Me_2NCH_2CH_2NH_2)_2$] complex, the complex-DNA binding ability was also performed in this study.

2. Material and Methods

2.1.Material

All the chemicals used in the study were available from Sigma.

2.2. Synthesistrans-[$CuBr_2(Me_2NCH_2CH_2NH_2)_2$]

2 mmol of $CuBr_2.2H_2O$ were placed in 10 ml methanol in ultrasonic for 10 min. Then, 4 mmol of N,N-dimethylethylenediamine were dissolved in minimum water solvent (1 ml). The two solutions were mixed together under ultrasound mode of radiation until the brown solution turned to full blue colour in a period 30 min. The reaction mixture was left to be evaporated at RT for two days. The blue powder was collected and washed well by THF with 85% yield.

2.3. Computational analysis

The *trans/cis* QM calculations parameter of the desired complex were performed by the GAUSSIAN09 with DFT/B3LYP 6-31G(d) basis set [18].

2.4. DNA-binding protocol

DNA absorption binding was carried out at pH 7.2, in Tris–HCl buffer/5mM Tris–HCl, 50 mMNaCl using [Cu] = 1.0×10^{-3} and [DNA]: 0.0,1.0×10^{-4},5.0×10^{-5},1.0×10^{-3}, 1.0×10^{-2} M.1.0×10^{-5} M. The full Cu(II)-DNA binding was carried out using recent published work [2].

2.5 Viscosity estimation

The viscosities of fixed [DNA] = 1.0×10^{-4} M, with different concentrations of [Cu(II)]: 0.0,1.0×10^{-6},2.0×10^{-6},5.0×10^{-6}, 7.0×10^{-6}, 1.0×10^{-5},2.0×10^{-5},3.5×10^{-5} and 5.0×10^{-5} Mwere estimated. $(\eta/\eta^{\circ})^{1/3}$ was plotted against [Cu(II)/DNA].

3. Results and discussion

3.1 Complexes

Under ultrasonic mode of radiation in ethanolic/water medium, neutral *trans*-[$CuBr_2(Me_2NCH_2CH_2NH_2)_2$]complex was prepared using *N,N*-dimethylethylenediamine as asymmetrical diamine ligands, the appearance of sky blue colour confirmed of the formation of the desired complex (Scheme 1).

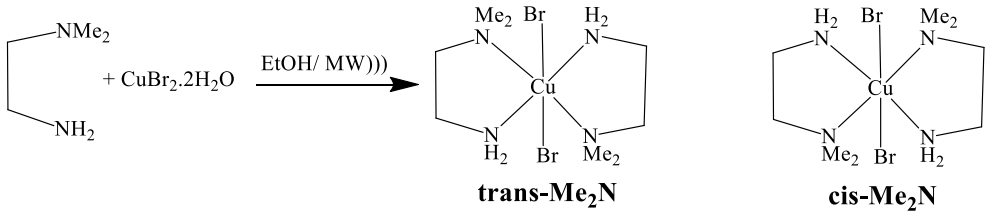

Scheme1: Synthesis of desired complex.

The complex is soluble in alcohols as EtOH, water and DMSO. However, insoluble in CH_2Cl_2, THF, acetone and non-polar solvents as dimethyl-ether.The desired complex is suggested as a neutral dibromo-octahedral salt complex. The nature of the complex was characterized by conductivity, solubility, elemental, and spectral analyses. Thermal (TG/DTG) and DFT-optimizations were investigated to determine the structural formula of the desired complex.

3.2. Optimization of cis/trans isomerization

The molecular structure geometries of the *trans* and *cis*-Me_2N-*stero*isomers [$CuBr_2(Me_2NCH_2CH_2NH_2)_2$] of the desired complex have been optimized in gaseous state at DFT/B3LYP6-31G(d) level of theory. The optimized structures are illustrated in Fig. 1; some computed parameters are listed in Table 1.

The steric hindrance of the four methyl groups of diamine ligands made the *trans*-Me_2N-isomer more favored over the *cis* one. The DFT-B3LYP total energy values are also consistent with such suggestion. For example, E_{B3LYP} for*cis*-isomer = -7291.74091956 a.u which is slightly higher than the *trans*-isomer (E_{B3LYP} for*trans*-isomer = -7291.75435934 a.u). Therefore, *trans* isomer is considered to be the kinetic favored isomer (most stable), while the *cis*-isomer is the thermodynamic favored one. Moreover, due to the steric effect of the Me groups in the cis isomer and to minimize the internal structure repulsion, one of bromide-copper bond (Br-Cu) was elongated to ~ 3.6 Å compared to ~ 2.7 Å in the same bond of the *trans*-isomer, the same bonds were

forced to bent far away from it linearity with Br-Cu-Br angle ~160 (°) compared to ~180 (°) same angle in the *trans*-isomer.

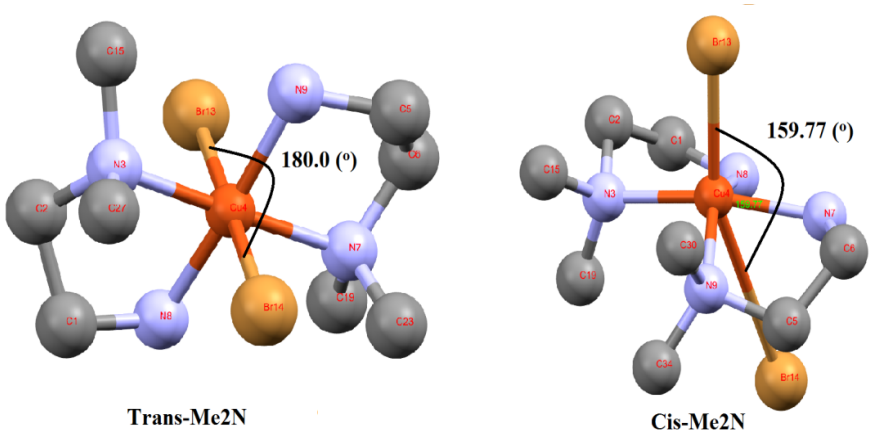

Figure 1:Optimization of *trans* and*cis*-[$CuBr_2(Me_2NCH_2CH_2NH_2)_2$]isomersof the desired complex at B3LYP/6-31G(d) level of theory**.**

Table1: Calculated total energy of *trans and cis*isomers of the desired complex

	***Cis*-Me2N**	***Trans*-Me2N**
E(UB3LYP)	-7291.74091956 a.u.	-7291.75435934 a.u.
RMS Gradient Norm	0.00002521 a.u.	0.00000276 a.u.
Dipole Moment	3.3045 Debye	0.1282 Debye
Point Group	C1	C1

3.3. Trans-isomer optimized structural parameters

Since the DFT reflected the *trans*- isomer as more stable one, the optimization geometric parameters were illustrated as shown in Tables 2 and 3. The structural parameters like bond lengths and angles (Tables 2) and dihedral angles (Tables 3) were performed on B3LYP 6-31G(d) level of theory.

Table2: Experimental bonds lengthsÅand angles values (°) of [$CuBr_2(Me_2NCH_2CH_2NH_2)_2$]

Bond No.	**Bond type**		**Bond value [Å]**	**Angle No.**	**Angle type**			**Angle value (°)**	**Angle No.**	**Angle value (°)**			**Angle value (°)**
1	C1	C2	1.5217	1	C2	C1	N8	104.78	17	N9	Cu4	Br14	109.57
2	C1	N8	1.5013	2	C2	N3	C15	106.08	18	N9	Cu4	Br13	70.4
3	C2	N3	1.5179	3	C2	N3	C27	108.26	19	N9	Cu4	N7	84.11
4	N3	C15	1.5153	4	C2	N3	Cu4	105.39	20	Br14	Cu4	Br13	179.98
5	N3	C27	1.5146	5	C15	N3	C27	106.35	21	Br14	Cu4	N7	100.41
6	N3	Cu4	2.136	6	C15	N3	Cu4	118.86	22	Br13	Cu4	N7	79.58
7	Cu4	N8	1.9371	7	C27	N3	Cu4	111.41	23	C6	C5	N9	104.78
8	Cu4	N9	1.9373	8	N3	Cu4	N8	84.12	24	C5	C6	N7	108.73
9	Cu4	Br14	2.5706	9	N3	Cu4	N9	88.94	25	Cu4	N7	C6	105.38
10	Cu4	Br13	2.74	10	N3	Cu4	Br14	100.42	26	Cu4	N7	C19	118.86
11	Cu4	N7	2.1364	11	N3	Cu4	Br13	79.59	27	Cu4	N7	C23	111.41
12	C5	C6	1.5217	12	N3	Cu4	N7	159.17	28	C6	N7	C19	106.08
13	C5	N9	1.5013	13	N8	Cu4	N9	140.8	29	C6	N7	C23	108.26
14	C6	N7	1.5178	14	N8	Cu4	Br14	109.62	30	C19	N7	C23	106.35

15	N7	C19	1.5153	15	N8	Cu4	Br13	70.4	31	C1	N8	Cu4	111.08
16	N7	C23	1.5146	16	N8	Cu4	N7	88.92	32	Cu4	N9	C5	111.07

Table3: Experimental dihedral angles (°) of $[CuBr_2(Me_2NCH_2CH_2NH_2)_2]$.

Angle No.	Dihedral angle type				Torsion value (°)	Angle No.	Dihedral angle type				Torsion value (°)
1	C2	C1	N8	Cu4	48.39	25	N3	Cu4	N9	C5	176.5
2	C1	C2	N3	C15	162.24	26	N8	Cu4	N9	C5	-104.15
3	C1	C2	N3	C27	-83.96	27	Br14	Cu4	N9	C5	75.82
4	C1	C2	N3	Cu4	35.35	28	Br13	Cu4	N9	C5	-104.17
5	C2	N3	Cu4	N8	-7.07	29	N7	Cu4	N9	C5	-23.16
6	C2	N3	Cu4	N9	134.29	30	N3	Cu4	N7	C6	64.06
7	C2	N3	Cu4	Br14	-116	31	N3	Cu4	N7	C19	-54.6
8	C2	N3	Cu4	Br13	64.02	32	N3	Cu4	N7	C23	-178.75
9	C2	N3	Cu4	N7	64	33	N8	Cu4	N7	C6	134.3
10	C15	N3	Cu4	N8	-125.74	34	N8	Cu4	N7	C19	15.64
11	C15	N3	Cu4	N9	15.63	35	N8	Cu4	N7	C23	-108.51
12	C15	N3	Cu4	Br14	125.34	36	N9	Cu4	N7	C6	-7.07
13	C15	N3	Cu4	Br13	-54.64	37	N9	Cu4	N7	C19	-125.73
14	C15	N3	Cu4	N7	-54.66	38	N9	Cu4	N7	C23	110.12
15	C27	N3	Cu4	N8	110.12	39	Br14	Cu4	N7	C6	-115.94
16	C27	N3	Cu4	N9	-108.52	40	Br14	Cu4	N7	C19	125.4
17	C27	N3	Cu4	Br14	1.19	41	Br14	Cu4	N7	C23	1.25
18	C27	N3	Cu4	Br13	-178.78	42	Br13	Cu4	N7	C6	64.03
19	C27	N3	Cu4	N7	-178.81	43	Br13	Cu4	N7	C19	-54.63
20	N3	Cu4	N8	C1	-23.15	44	Br13	Cu4	N7	C23	-178.78
21	N9	Cu4	N8	C1	-104.18	45	N9	C5	C6	N7	-54.45
22	Br14	Cu4	N8	C1	75.84	46	C6	C5	N9	Cu4	48.4
23	Br13	Cu4	N8	C1	-104.17	47	C5	C6	N7	Cu4	35.35
24	N7	Cu4	N8	C1	176.51	48	C5	C6	N7	C19	162.24
						49	C5	C6	N7	C23	-83.96

3.4. Ms, EDX, CHN-analyses and molar conductivity

MS (m/z) exhibited the charged ion at 395.2 $[M-H]^+$Calcd. for$C_8H_{24}Br_2CuN_4$, to be 396.9 for theoretical value that is consistent with molecular formula. The EDX analysis of the desired complex reflected the atomic content of the molecule; no strange atoms out of the expected molecular formula were detected, as seen in Fig.2. The presence of Br, Cu, C, N and traces of O elements in the lattice of the molecule were confirmed as shown in Fig.2.

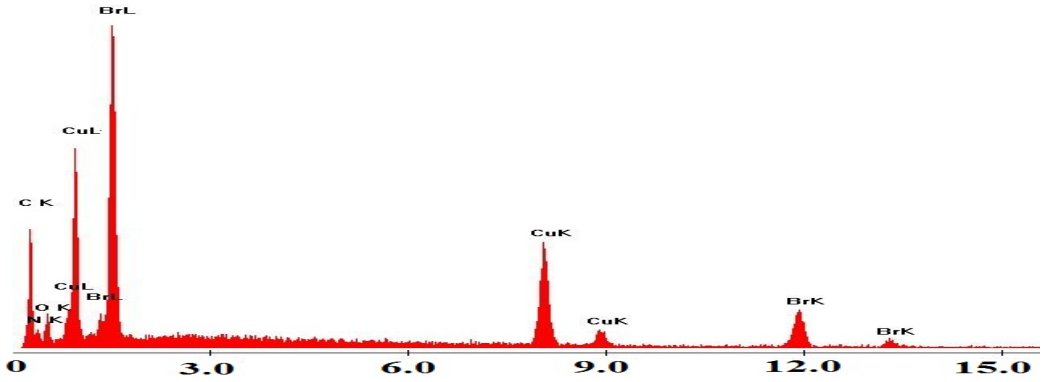

Figure 2: EDX spectrum of $[CuBr_2(Me_2NCH_2CH_2NH_2)_2]$ complex.

Elemental analyses of the desired complex experimentally reflected the total atomic content as: C, 23.12; H, 6.19 and N, 13.38, calculated : C, 23.01; H, 6.27 and N, 13.41, the result is consistent with $[C_8H_{26}Br_2CuN_4O]$ (with one H_2O) formula more than that of $[C_8H_{24}Br_2CuN_4]$ theoretical atomic content: C, 24.04; H, 6.05 and N, 14.02, such calculations strongly support the presence of only one water molecule in the lattice of complex reflectiong $[CuBr_2(NN)_2].H_2O$ as general formula.
The molar conductivity $\Lambda_M$found to be 95 Scm^2/mol when $1x10^{-3}$ M of complex was dissolved in 100 ml water, this value confirmed the neutral nature of the complex as well as [1:2] of M to L molar ratio.

3.4. FT-IR and DFT-IR

Both experimental and calculation frequency vibration of the functional groups in the desired complex were performed, as seen inFig.3.

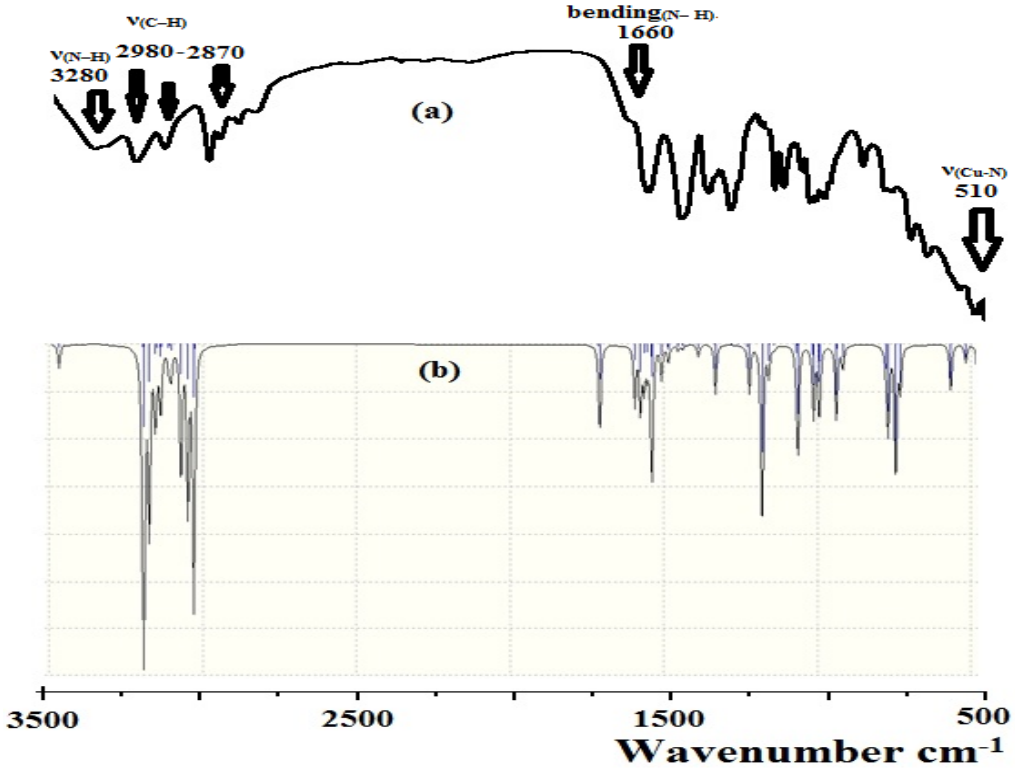

Figure 3: (a) Experimental FT-IR and (b) DFT/B3LYP 6-31G theoretical vibration spectra of the desired complex.

The complexreflected experimentally and theoretically several peaks belong to vibrations mode of each functional group. For example, water $\nu_{(HO-H)}$ was detected only experimentally (exp. = 3450 cm^{-1} while DFT = not detected), $\nu_{(N-H)}$, (exp. = 3280 cm^{-1}, DFT = 3465 and 3460 cm^{-1}), $\nu_{(C-H)}$(exp. = 2980 and 2870 cm^{-1} while DFT = 3150 and 3060 cm^{-1}), bending$_{(N-H)}$, (exp. = 1660 cm^{-1} while DFT = 1710 cm^{-1}), and $\nu_{(Cu-N)}$(exp. ~ 510 cm^{-1} while DFT = 550 cm^{-1}).

The obtained DFT computed IR spectra reflected an overestimated result compared to the experimental one due to the different electron correlation and unharmonicity effects in the real system [18-20]. In general, the graphical correlation (R^2 = 0.95) revealed an acceptable overall matching between experimental and theoretical IR results.

The complex in water showed two types of absorption at 25 ^{o}C.The first one was sharp and in the UV-region with λ_{max} = 255 nm which was attributed to π - π^* electron transition (Fig. 4a). The second one was broad band in the visible region (blue colour) with λ_{max} = 595 nm due to d to d electron transfer, as recorded in Fig. 4b.

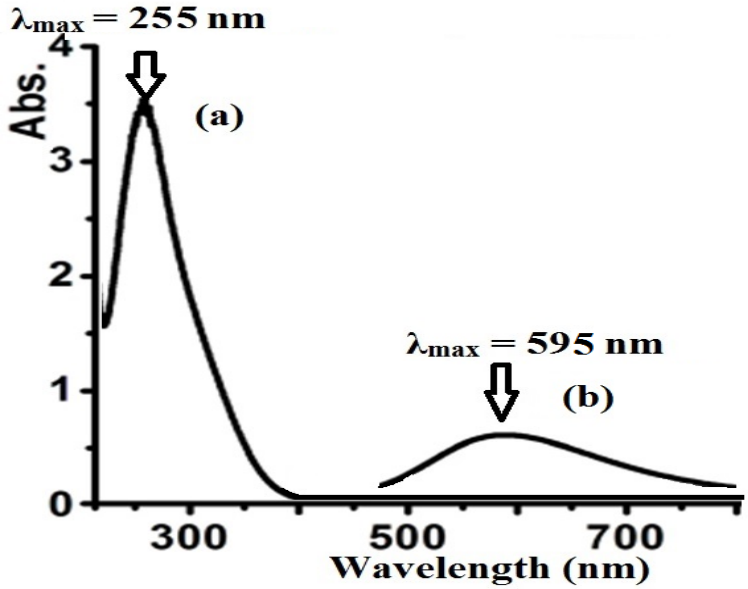

Figure 4:RTUV-Vis. Abs. behaviour of the complex dissolved in water, (a) 1×10^{-5} M and (b) 5×10^{-4}M.

3.5. MEP of trans-[$CuBr_2(Me_2NCH_2CH_2NH_2)_2$]

MEP computation analysis is quite helpful to figure out the electrophilic and nucleophilic positions in the desired complex. In this work, MEP/B3LYP for *trans*-[$CuBr_2(Me_2NCH_2CH_2NH_2)_2$]was carried out in gaseous state, as seen in Fig. 5. The electrostatic potential was evaluated by color and intensity difference as in the following order red>orange>yellow>green>blue. The bromide ions recognized by deep-red color as the highest negative atoms, proton of the nitrogen (H-N amine) reflected a blue color as the lowest in negative charge (acidic proton), other functional groups showed light blue to green color reflected a medium in their electrostaticity.

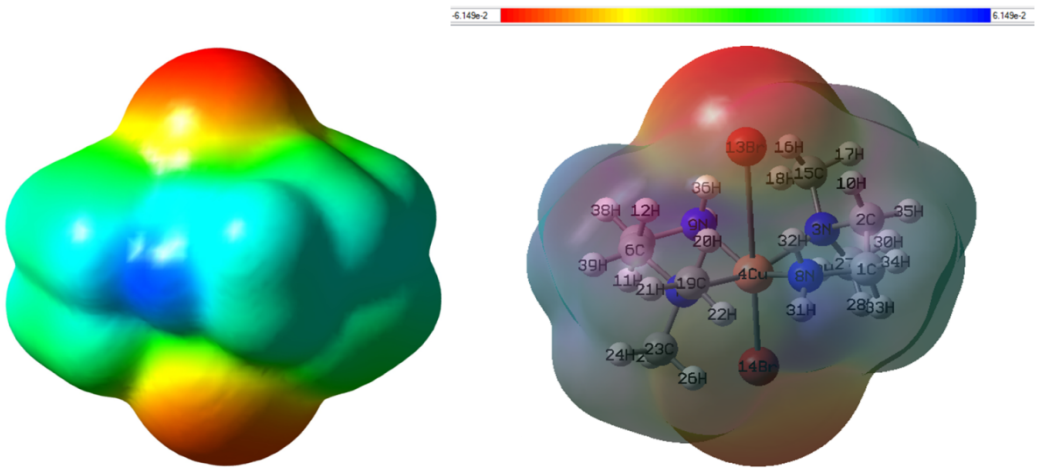

Figure 5: MPE *trans*-[$CuBr_2(Me_2NCH_2CH_2NH_2)_2$]

3.6. Thermal decomposition

TG/DTA (Fig. 6) was used to evaluate the thermal stability of the *trans*-[$CuBr_2(Me_2NCH_2CH_2NH_2)_2$] complex in an open atmosphere and 10 ^{o}C/min rate of heat. In range 0-1000^{o}C the TG reflected three main

thermal steps ended by metal oxide formation started by dehydration followed by complex-ligands destruction. The dehydration step performed in 60 to 80 ^{o}C (with 4% wt. lost). This signalized the one water molecule crystallized and not coordinated in the lattice of the complex [1-4]. The anhydrous complex is stable over 80-230 °C temperature range and decomposed from 230 to 290 ^{o}C losing ~ 48% of weight due to $Me_2NCH_2CH_2NH_2$ ligands de-structured from the complex to produce pure $CuBr_2$ which was stable up to 410^{o}C. As final product of third step CuO, with 16% wt. was formed through a composited one step were bromides de-structured and oxide combined over a broad arrangement of 410-560 ^{o}C (with 44% wt. lost).

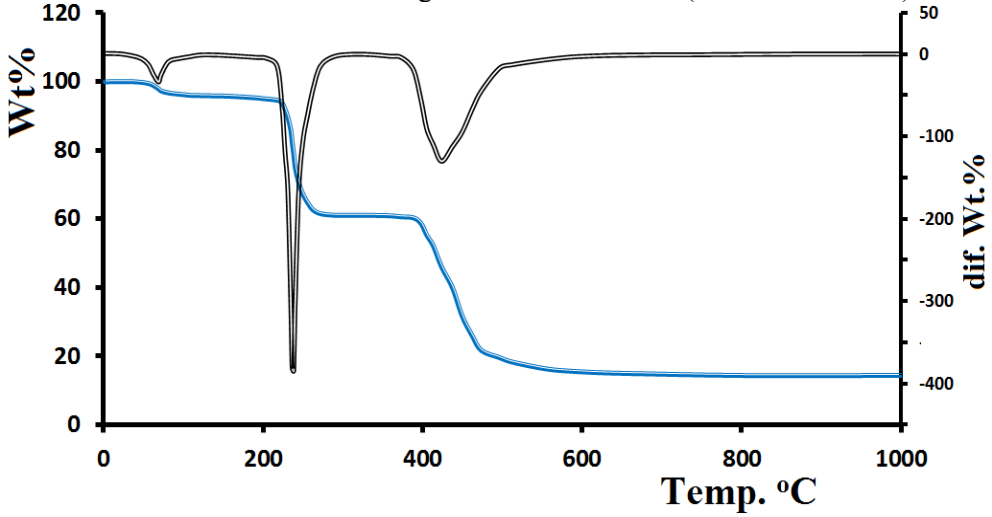

Figure 6:TG/DTG of *trans*-$[CuBr_2(Me_2NCH_2CH_2NH_2)_2$ complex**.**

3.7. Absorption spectroscopy titration (DNA binding)

To figure out the binding ability of *trans*-$[CuBr_2(Me_2NCH_2CH_2NH_2)_2]$complex with the DNA, as a sensitive and powerful technique the absorption spectroscopy titration was performed [2-12]. DNA binding with the complex was performed in the visible region; the $K_b$binding constantwas also evaluated in order to esteem the DNA binding mode and its strength. Current works proposed that the DNA bind the drugs due to π–π stacking interactions between the DNA base pairs and functional group in the backbone of the complexes cased hypochromism or bathochromism shift which supported intercalative binding type [2]. The absorption spectra of *trans*-$[CuBr_2(Me_2NCH_2CH_2NH_2)_2]$ in the presence and absence of the CT-DNA are presented in Fig.7. The existence of a band at 595 nm, indicates a significant lowering in absorption of the complex which was detected by raising the DNA concentrations [2].

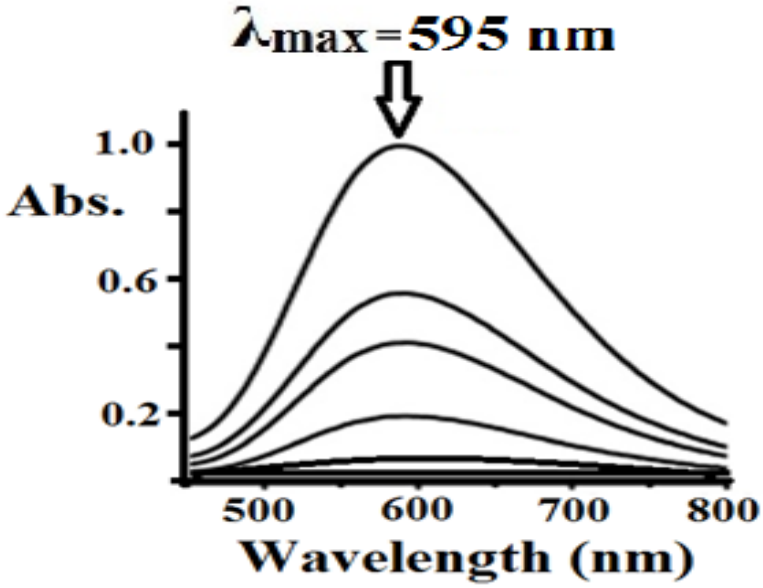

Figure 7: Absorption titration spectra of *trans*-$[CuBr_2(Me_2NCH_2CH_2NH_2)_2]$complex with CT-DNA at 595 nm in Tris-HCl buffer; [Cu] = 1.0×10^{-3}; [DNA]: 0.0,1.0×10^{-4},5.0×10^{-5},1.0×10^{-3}, 1.0×10^{-2} M. The arrows denoted the imperceptible decrease on *trans*-$[CuBr_2(Me_2NCH_2CH_2NH_2)_2]$concentration by DNA increment.

Plotting [DNA] *vs.* [DNA]/(εa-εf) using the equation 1, enable us to calculate the K_b constant. The K_b value of the complex was found to be 5.0×10^4 M^{-1} which is consistent with the reported data [2].

$$[DNA]/(\epsilon_a - \epsilon_f) = [DNA]/(\epsilon_b - \epsilon_f) + 1/K_b(\epsilon_b - \epsilon_f) \quad \text{.....1}$$

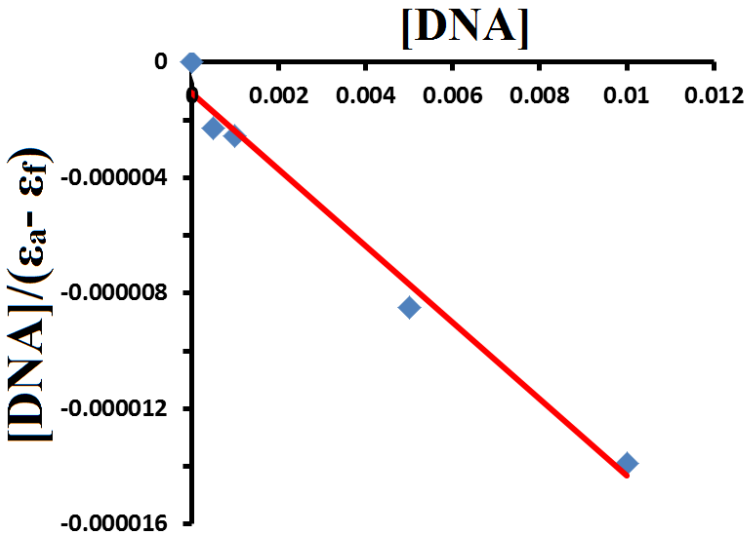

Figure 8: Plotting of [DNA] *vs.* [DNA]/(ε_a- ε_f) at λ_{max} = 595 nm to evaluate the K_b value.

3.8. Viscosity test

The [Cu:DNA] binding method of the desired *trans*-[$CuBr_2(Me_2NCH_2CH_2NH_2)_2$] complexes was additionally confirmed by viscosity evaluations. The effect of the *trans*-[$CuBr_2(Me_2NCH_2CH_2NH_2)_2$] concentrations on the DNA-viscosity were performed under fixed concentration of [DNA] = 1.0×10^{-4} M, with different concentrations of complex, [Cu(II)]: 0.0,1.0×10^{-6},2.0×10^{-6},5.0×10^{-6}, 7.0×10^{-6}, 1.0×10^{-5},2.0×10^{-5},3.5×10^{-5} and 5.0×10^{-5} M as illustrated in Fig.9. Conventional [M:DNA] intercalative coordination fashionproposed that: DNA-helix as base pairs ligands should be extended by coordinating with the metal ions complexes causing an increase in the DNA viscosity [2, 3, 4-12].

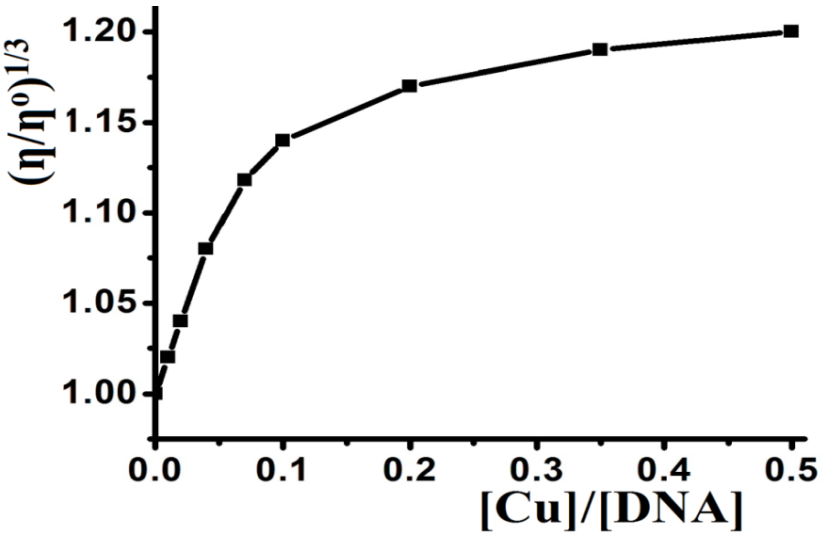

Figure 9: RT effect of difference *trans*-[$CuBr_2(Me_2NCH_2CH_2NH_2)_2$] complex concentrations on the relative viscosities η^o of $1.0x10^{-4}$ M of CT-DNA.

Increasing Cu(II) complex concentrations revealed a non-linear raise in the DNA relative viscosities which reflected its affinity to bind DNA. The proposed outcome of such complex binds the DNA strongly through the intercalation mode of coordination.

Conclusions

Trans-[$CuBr_2(Me_2NCH_2CH_2NH_2)_2$] neutral complex was prepared under ultrasonic mode of radiation in a very good yield. The DFT-optimization was performed to calculate the structure parameters. The MS, EA, EDX, conductivity, UV-vis. and TG-thermal analysis were performed to estimate the complex real structure. EDX, EA, IR and TG revealed the total composition of the complex and supported the $[CuBr_2(NN)_2].H_2O$ general formula. The conductivity and solubility tests supported the neutral nature of the complexes. TG/DTG reflected the complex as neutral di-bromide high stability complex decomposed through three steps mechanism. The UV-Vis. analysis supported the octahedral geometry formation around the Cu(II) centre. The absorption and viscosity measurements reflected the complex as very good DNA binder. K_b intercalation binding mode showed the complex as strong DNA binder.

References

1. H. Qian, Z. Chu, W. Huang, J. Liu, *J. Mol. Struct.* 840 (2007) 38–43.
2; I. Warad, F. F. Awwadi, M. Daqqa, A. Al Ali, T. S. Ababneh, T. M.A. AlShboul, T. M.A. Jazzazi, F. Al-Rimawie, T. B. Hadda, Y.N. Mabkhot, *J. Photochem. Photobiol. B: Biol.* 171 (2017) 9–19.
3; F. A. Saleemh, S. Musameh, A. Sawafta, P. Brandao, C. J. Tavares, S. Ferdov, A. Barakat, A. Al Ali, M. Al-Noaimi, I. Warad, *Arab. J. Chem.* 10 (2017) 845–854.
4. I. Warad, Y. Al-Demeri, M. Al-Nuri, S. Shahwan, M. Abdoh, S. Naveen, N. K. Lokanath, M. S. Mubarak, T. B. Hadda, Y. N. Mabkhot, *J. Mol. Struct.* 1142 (2017) 217–225.
5. M. Al-Noaimi, M. I. Choudhar, F. F. Awwadi, W. H. Talib, T. B. Hadda, S. Yousuf, A. Sawafta, I. Warad, *Spectrochim. Acta Mol. Biomol.Spectrosc.* 127 (2014) 225–230.
6. S. Jana, S. Bhowmik, K. Harms, A. Bauzá, A. Frontera, Sh. Chattopadhyay, *Inorg. Chim.Acta* 451 (2016) 16–22.
7. P. Sureshbabua , A.S. Tjakraatmadjab, C. Hanmandlua , K. Elavarasana, N. Kulak, S. Sabiaha, *RSC Adv.* 29 (2015) 22405-22418.
8. S.S. Wu, W.B. Yuan, H.Y. Wang, Q. Zhang, M. Liu, K.B. Yu, *J. Inorg. Biochem.* 102 (2008) 2026–2034.
9. L. Rostami, H. Golchoubian, *Inorg. Chim.Acta* 462 (2017) 215–222.
10. H. Golchoubian, G. Moayyedi, N. Reisi, *Spectrochim. Acta Mol. Biomol. Spectrosc.*138 (2015) 913–924.
11. I. Warad, M. Azam, S. I. Al-Resayes, M. Shahidu, I. Sarfaraz, A. Salim, F. Haddad, *Res. Chem. Intermed.* 42 (2016) 379–389.
12. A. Barakat, S. M. Soliman, H. A. Ghabbour, M. Ali, A. M. Al-Majid, A. Zarrouk, I. Warad, *J. Mol. Struct*.1137 (2017) 354–361.
13. A. Barakat, A. M. Al-Majid, M. Sh. Islam, I. Warad, V. H. Masand, S. Yousuf, M. I. Choudhary, *Res. Chem. Intermed.* 42 (2016) 4041–4053.
14. M. Al-Noaimi, A. Nafad, I. Warad, R. Alshwafy, A. Husein, W. H. Talib, T. B. Hadda, *Spectrochim. Acta Mol. Biomol.Spectrosc.* 122 (2014) 273–282.
15. M. Al-Noaimi, M. Choudhar, F. Awwadi, W. Talib, T. B. Hadda, S. Yousuf, A. Sawafta, I. Warad, *Spectrochim. Acta Mol. Biomol.Spectrosc.*127 (2015) 225-232.
16. M. Azam, I. Warad, S. Al-Resayes, N. Aldzaqr, M. Kha, R. Pallepogu, S. Dwivedi, J. Musarrat, M. Shaki*J. Mol. Struct.* 1047 (2013) 48–54.
17. A. Janim, M. Al-Nuri, A. BaniOdeh, S. A. Barghouthi, M. Ayesh, A. Al Ali, S. Amereih, I. Warad, *J. Mater. Environ. Sci.* 7 (2016) 3447-3453.
18. K. Fukui, *Science* 218 (1982) 747-750.
19. J. Aihara, *J. Phys. Chem. A* 103 (1999) 7487-7493.
20. A. K. Singh, S. K. Pandey, O. P. Pandey, S. K. Sengupta, *J. Mol. Struct.* 1074 (2014) 376-382.

(2018) ; http://www.jmaterenvironsci.com